Could converter domination lead to better voltage stability in AC transmission? - an overview

Chen, Dong; Zhang, Zehua

Published in:
2021 IEEE 1st International Power Electronics and Application Symposium (PEAS)

DOI:
10.1109/PEAS53589.2021.9628595

Publication date:
2021

Document Version
Author accepted manuscript

Could Converter Domination Lead to Better Voltage Stability in AC Transmission? - An Overview

Dong Chen
Department Electrical and Electronics Engineering
Glasgow Caledonian University
Glasgow, UK
dong.chen@gcu.ac.uk

Zehua Zhang
Department Electrical and Electronics Engineering
Glasgow Caledonian University
Glasgow, UK
Zehua.Zhang@gcu.ac.uk

***Abstract*— In this paper, an overview is conducted on the prospected "net-zero" transmission network. A review of existing root-mean-square approach in voltage stability analysis is carried out in the first place. By introducing the control paradigms of converter control for modern and future sources of renewable energy and storages, limitations of root-mean-square has been discussed. After that, an electromagnetic approach in enhancing voltage stability is illustrated. With a case study of converter domination, a counter example is presented to showcase such electromagnetic enhancement can break through the Hoff bifurcation limit set by root-mean-square representation in voltage stability with single-infinite benchmark. Finally, it is concluded that converter domination can bring about better voltage security than state-of-the-art.**

Keywords—voltage stability, root-mean-square, bifurcation, voltage sensitivity, converter domination, electromagnetic transient

I. INTRODUCTION

To combat the climate change and assist the post-COVID economic recovery, the shift towards a "net-zero" carbon emission power system is becoming as global interest. To make it happen by 2050, renewable energy, wind energy inpaticular, are supposed to be the main source to power the transmission network from the generation side in GB power network [1]. Apart from direct integration of wind turbines and photovoltaic systems, High Voltage Direct Current (HVDC) inter-connector and energy storage systems are expected to provide services of indirect integration and power/energy reserve in a "Net-zero" transmission network. To date and in foreseeable future, renewable generations, HVDC and storage systems are going to be interfaced by power electronics converters as well [2]. As a result, the existing domination of synchronous generators are going to be gradually taken over by converter; hence the terminology of converter domination.

The challenge of powering an electricity network with zero emission is not only about balancing the intermittency of generations, but also concerns the transmission capacity of delivering bulk renewable power over distance. Expansion of AC transmission limit can effectively prevent failure of transmission and therefore is desirable for system operators and planners.

Voltage instability occurs when the designated operating point is heading into an unstable region, where a perturbation will lead to excessive oscillations or voltage deviations [3]. If irrelevant constraints are disregarded, such as thermal constraints, non-linear controls, i.e., forced saturation, switching of control mode, operation of switch gear, tap changing of transformer, etc., power transmission can be characterized by differential equations in respect of time. The mathematical boundary of unstable region can be defined by bifurcations, namely Hoff Bifurcation and Saddle Node Bifurcation [4].

Assuming the electromagnetic transients are negligible, Root Mean Square (RMS) representations, or equivalently regarded as power flow or phasor representations, are employed to interpret the mechanism of voltage instability in single-infinite bus benchmark [4][5] and then extended to assessment of multi-bus systems and corresponding mitigation approaches [6]. Such assumption is valid for power system dominated by synchronous machines as the coupled inertia of turbines will adequately filter out fast Electromagnetic (EMT) dynamics.

However, RMS representation has been found inadequate for converter domination, especially for Voltage Source Converters (VSCs), which are based on fast reacting power electronics devices [7]. With heavy inertia removed under converter domination, the dynamics of VSC are driven by control loops feedback by instantaneous EMT measurements and their dynamics. As a result, EMT approaches have to be adopted to analyse and mitigate possible voltage instability in the context of converter domination. And this is leading to new behaviours of power system, which have not been clearly understood in power system planning and operation with RMS representations.

In the rest of the paper, an overview will be provided on voltage stability towards converter domination. In section II, a review will be carried out on the basic principle of voltage instability for a power system dominated by synchronous machines. It will review the principles of voltage stability analysis with RMS representations. In section III, the scenario of converter dominated transmission and the EMT control of voltage source converter will be introduced. In section IV, the latest development in enhancing voltage stability with EMT approach is introduced in principle, and then illustrated with an example which showcase how EMT control can make a breakthrough of transmission limit set by RMS voltage stability. Finally, cconclusions are drawn in Section V.

II. REVIEW OF VOLTAGE STABILITY WITH RMS REPRESENTATION

Assuming the operating frequency is very close to the fundamental frequency, the mechanism of voltage instability can be typically interpreted with a benchmark of 2-bus system using Thevenin Equivalent, which is shown Fig. 1 (a), where the grid is represented by a grid source in series with a grid impedance. The static limit of power transmission, which corresponds to the operating point when the system starts to lose real solution to power flow equilibrium, is set by Saddle-Node Bifurcation. At the bus of interest in Fig. 1(a), the loss of equilibrium can be electrically interpreted by the principle of impedance matching. That is, to enable power delivery, the

apparent impedance of the interested load bus must be greater than the apparent impedance connected to the grid source [9]

$$|Z_{eq2}| > |Z_{eq1}| \quad (1)$$

, where $Z_{eq2} = R_{eq2}+jX_{eq2}$ are the equivalent impedance of the operating load. This mechanism is demonstrated in Fig. 1(b). Alternatively, the power flow in Fig. 1(a) can also be expressed by a quadratic equation as

$$(PX_1 + QR_1)^2 + (V^2 - QX_1 + PR)^2 - (EV)^2 = 0 \quad (2)$$

, where $Z_{eq1} = R_1 + jX_1$ and the condition to secure existence of a solution to an equilibrium voltage is

$$\Delta = (-2PR_1 - 2X_1Q + E^2)^2 - 4[(RQ + X_2P)^2 + (-PR_1 + X_1Q_1)^2] \geq 0 \quad (3)$$

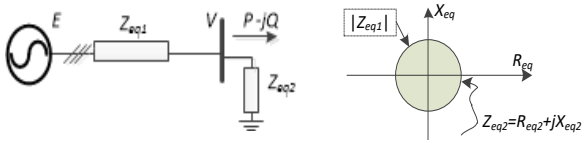

(a) 2-bus system schematic (b) Static impedance matching

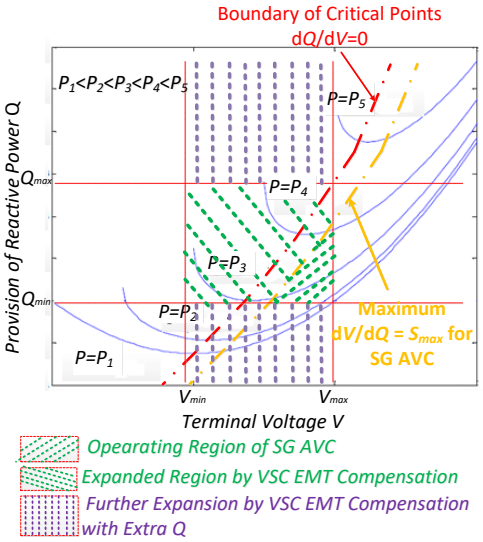

(c) RMS voltage dynamics of 2-bus transmission line in *Q-V* Plane

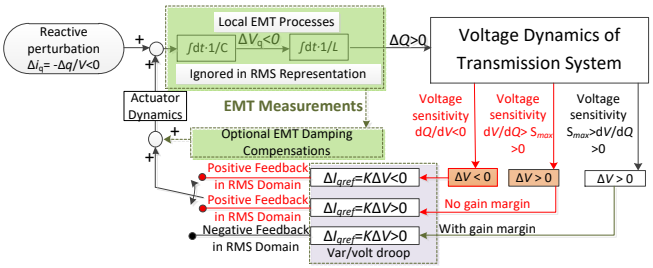

(d) Voltage dynamics with var/volt droop

Fig. 1 Voltage Stability in RMS Representation

It can be inferred from Fig. 1(b) and (1) that, the mathematical limit of active power transmission is determined by the metrics of electrical network. Convenient enough to explain the mechanism, the approach of static impedance matching does not go far in a complex network as the equivalent impedance is difficult to obtain in reality. Practically, this limit has rarely been exhausted, which is to prevent oscillations caused by the dynamic interactions among grid strength, generations and sinks.

The grid strength, which is a regional index, are generally defined as the ability at the point of connection to maintain its voltage during the injection of reactive power [8]. In this sense, it can be mathematically represented by voltage sensitivity in respective of reactive power, i.e. d*V*/d*Q*, in RMS domain [4][5]. As is shown by the *Q*-*V* curve in Fig. 1 (c), the blue solid curves represents the operating trajectories for various active power load *P* in Fig. 1(a). The region associated with negative value of d*V*/d*Q* are traditionally defined as the forbidden region, i.e. the left hand side of the boundary curve d*Q*/d*V* = 0 (red dashed line) in Fig. 1(c). This dynamic limit is driven by the fact that all reactive compensation/control schemes are designed based on a presumed positive voltage sensitivity d*V*/d*Q* [5]; any disturbance to an equilibrium with the region of d*V*/d*Q*<0 will lead to positive feedback and consequent instability in Automatic Voltage Control (AVC). When an operating point is crossing this boundary curve towards the region of the left-hand side, the real part of at least one eigen value of the system will become positive, where a Hoff bifurcation is occurring.

In reality, when a primary AVC, i.e. var/volt droop, is in place, a great value of d*V*/d*Q*, illustrated as the yellow curve in Fig. 1(c), may have already led to oscillations, i.e. Hoff bifurcation, before the boundary of d*Q*/d*V* = 0 is reached, due to poor gain margin. This further reduces the operational region of a system configured by RMS representations. This instability against Hoff bifurcation can also be interpreted by the block diagram Fig. 1(d) with perturbation analysis. As shown in Fig. 1(d), when a negative perturbation of instantaneous $\Delta i_q < 0$ is injected to the transmission system from the bus of interest into the grid, it will introduce a positive change to reactive power (capacitive) $\Delta Q > 0$ (when the EMT dynamics are ignored). This positive ΔQ will lead to a change of voltage magnitude ΔV as a response from the transmission system. According to the Fig. 1(c), the voltage dynamics in RMS domain are sensitive to the operating point as follows:

(1) When the voltage sensitivity is in the region of d*V*/d*Q*<0, the local voltage response will be a negative voltage change $\Delta V<0$; this negative voltage change will lead to a negative output of reactive current compensation with a positive var/volt droop coefficient *K*. Implemented by the actuator, synchronous machine or VSC, the var/volt droop will end up as a positive feedback and amplify the perturbation, which leads to instability. This instability mechanism applies to all positive var/volt droops (*K*>0); hence the traditional forbidden region in *Q*-*V* curves.

(2) When the voltage sensitive is in the region of d*V*/d*Q* > S_{max} > 0, where S_{max} is the critical value of d*V*/d*Q* which corresponds to zero gain margin to a specific var/volt droop co-efficient *K*, although the change of local voltage is positive $\Delta V>0$, lack of gain margin in this closed-loop control will again end up as a positive feedback and voltage instability.

(3) Only when the voltage sensitivity in the region of 0 < d*V*/d*Q* < S_{max}, the perturbation can be effectively mitigated with negative feedback in RMS domain. When the constraints of operating limit of local voltage and reactive power are further considered as confining boudaries, the operating region is illustrated as the shaded area labelled as “Operating Region of SG AVC” in Fig. 1 (c).

To enable voltage security assessment for a meshed transmission network, both dynamic and static limits of

voltage stability have to be considered simultaneously. With the assist of circuit analysis, the impact of network metrics, along with generations and sinks, can be generically linearized and characterized as a matrix of 1st order partial derivatives, where Jacobi matrix can be derived or further reduced for voltage stability assessment [4][9][10][11][12][13]. Manipulating the property of Jacobian singularity as an essential indication of bifurcation [10][11] or the critical point of eigen values in modal analysis [12], a variety of methods have been derived to estimate, correct, or prevent voltage instability. However, such method cannot explicitly predict the exact point of Saddle Node Bifurcation, i.e. loss of equilibrium, before the operating point arrives in close vicinity. This is due to the lack of mathematical tool to analytically determine the existence of non-linear power flow solutions.

III. Overview of Voltage Source Converter Control

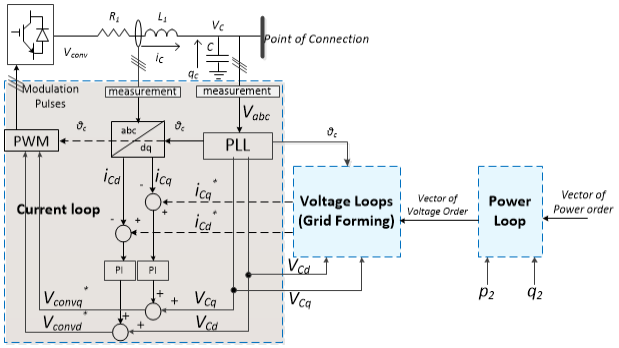

Fig. 2 Generic Control Strategy of a VSC [13]

Although the assumption of RMS modelling is generally valid for a power grid dominated by synchronous machines, as large inertia of synchronous turbines can filter/damp out the impact of EMT dynamics, it is not valid for converter domination. Unlike synchronous machines, modern renewable generators, HVDC inter-connectors, and battery storage systems are often interfaced by VSCs. With feedbacks of instantaneous quantities, i.e. voltage, currents, from local sensors in an order of kHz, the dynamics of converters are largely driven by their internal control over instantaneous EMT quantities. Those instantaneous quantities are locally controlled by manipulating the voltages and currents that are naturally held by capacitive and inductive elements, respectively. Depending on the application and strategy, the structures of VSC control scheme varies with different combinations of closed-loops [13].

A typical cascaded control strategy of a VSC is illustrated in Fig. 2 shows. The dynamics of EMT quantities under the control of VSC can be generalized as a first order plant as

$$J\frac{dx}{dt} = y \tag{4}$$

where y is the input to the plant, x the EMT quantity under control and J the constant of the "inertia" to hold the EMT quantity. By comparing the error between the desired value and measurement of x, the plant input, y , is kept adjusting to minimize the error with a regulator. When such process is quickly repeated, i.e. in an order of kHz or above, x is expected to be under tight control to follow the desirable value.

For instance, considering one inner current loop of a 3-phase VSC, x refers to the current component hold by VSC reactor, either in d-axis or q-axis, J the inductance value of L_1; and y is the corresponding instantaneous voltage across the inductive element of VSC reactor, which is in linear relationship with the modulated voltage of VSC. Thus, by quickly adjusting he modulated voltage of VSC, the current can be controlled to follow a given order. As to an outer voltage loop, x becomes one voltage component held by terminal capacitor, J the terminal capacitance value of C; and y becomes the corresponding charging current into the terminal capacitance, which is in a linear relationship with the current carried by VSC reactance. In this case, the current carried by VSC reactance can be used to adjust the capacitive voltage through current control as its "actuator".

When a VSC control is poorly damped, oscillatory behaviours may arise when integrating it to a power network. As these oscillatory frequencies may deviate significantly from the fundamental [8], the dynamics over broad frequencies must be captured in voltage stability analysis. Obviously, ignoring EMT dynamics means rejection of EMT control of converters and the associate oscillations over broad frequencies in stability assessment [15]; hence is no more valid for the assessment against Hoff bifurcation. In this sense, EMT dynamics must be included in the modelling to reflect the true limit of Hoff Bifurcation. For the practical implementation of state space modelling, or other equivalent analytical approach, the dynamics of charging/discharging inductive and capacitive elements must be inclusive along with the associate control.

Practically, not all the EMT loops illustrated in Fig. 2 are implemented in a VSC. Depending on the actual need, selective control loops illustrated in Fig. 2 can be cancelled or preserved. For example, when the voltage loops are completely cancelled, the control becomes a grid following control. Whereas, when inner current loops are cancelled, it becomes a strategy of so-called virtual synchronous machine [16].

Apart from the control over the vectors of power, voltage and current shown in Fig. 2, further auxiliary loops can be added between selected EMT states to reshape the dynamics of the system. In particular, auxiliary loops between EMT states can be created to improve the damping of an established control scheme [17][18].

On one hand, EMT quantities are insignificant in a power system dominated by synchronous machines; on the other hand, the large time constant brought by inertia also make it very difficult for synchronous machine to control fast EMT dynamics. As a result, EMT dynamics are ignored in traditional voltage stability as they are neither necessary to capture nor possible to control them in a power system dominated by synchronous machines; hence the use of RMS representation in voltage stability analysis.

This consequent RMS approach in voltage stability assessment overlooks not only the oscillations of broader frequencies due to poor design of converter control, but also the potential of an improved voltage stability that synchronous machines may not offer.

Due to the inevitable displacement between renewable sources and load centres, it is desirable to maximize the capacity and expansion of active power transmission under converter domination. While the physical transmission limit is ultimately determined by network metrics against Saddle Node Bifurcation, the operating limit set against Hoff

bifurcation of the overall system can be enhanced up to such physical limit.

Taking advantage of the flexibility of VSC control, enhancement of transmission limit can be achieved by improving EMT damping. As is shown in Fig. 1(d), if the local EMT dynamics, e.g. instantaneous capacitive voltages, or inductive currents, can be captured and appropriately compensated for the provision of active damping with the actuator, the transmission system can operate in the region of $dV/dQ > S_{max} > 0$ and $dV/dQ < 0$ so the capacity of power transmission is expanded. Following this principle, when the EMT measurements and actuator, i.e. VSC, are quick enough to capture the dynamics and actuate the damping compensation, the operational region can be expanded as Fig. 1(c) shows with the shaded area labelled as "Expanded Region by VSC EMT Compensation".

When the EMT damping is sufficient, a tighter regulation of local voltage, strong var/volt, towards the nominal value can be enabled and used to exhaust the transmission limit against Saddle Node bifurcation which is set by network metrics alone.

IV. Example of Expanding Transmission Limit with VSC-Domination

As an example, a benchmark system is set up as Fig. 3 to showcase how the Hoff bifurcation defined by RMS representation can be broken through by EMT damping. As shown in Fig. 3, a VSC-HVDC station is connected to a grid represented by a single-infinitive bus via a transmission line. A voltage regulation, i.e. var/volt droop, is embedded within the local control of VSC-HVDC station.

A second VSC, namely VSC stabilizer, is installed in a distance from the VSC-HVDC to expand the transmission limit against Hoff bifurcation, i.e. provide damping. Based on basic vector control of inner current loop with set values of zeros for both current components, the VSC stabilizer is equipped with an auxiliary control loop, i.e. partial grid-forming loop, to improve EMT damping [13]. Referring to Fig. 1(d), the input of the measurement to the EMT compensation is q-axis voltage V_{2q} at the stabilizer terminal and the output is the order of q-axis current of the 2nd VSC (VSC stabilizer), i_{cq2}*,. Referring to Section III and the generic control diagram in Fig. 2, the configurations of control loops of the 2 VSCs in Fig. 3 are summarized as Table I shows.

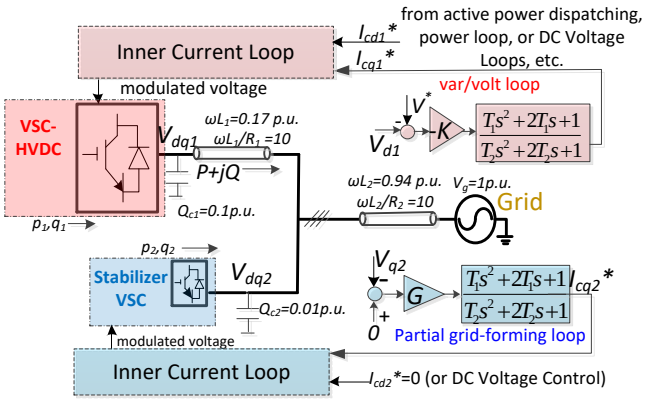

Fig 3 EMT Enhancement with a remote VSC Stabilizer

Tab I Control Loops of VSCs in Fig. 3

	Current Vector Loops	Voltage Vector Loops	Power Vector Loops	Auxiliary Loops
VSC-HVDC	Yes	No	active power loop only	Var/Volt Droop
VSC-Stabilizer	Yes	No	No	Partial grid-forming loop

When the VSC-HVDC is inverting/rectifying power to/from the grid with an *SC*R = 0.9 at *X*/*R* ratio of 10, the connection is extremely weak. With a var/volt droop (AVC) is applied, the eligible operating region in RMS representation can be generally represented by the green shaded area in Fig. 2(b) in *Q*-*V* plane and more specifically in Fig. 4 (left half) in *Q*-*P* plane. When the grid strength is very low and operating voltage must be confined to a limited variation, the active power will be capped well below the physical limit determined by Saddle Node Bifurcation due to Hoff bifurcation defined by RMS representation. By applying extra EMT stabilizer with a 2nd VSC as the stabilizer, shown in Fig. 3, the feedback control over the q-axis voltage of shunt capacitance can improve the damping of the overall system. As a resultant effect, the outputting power of the VSC-HVDC

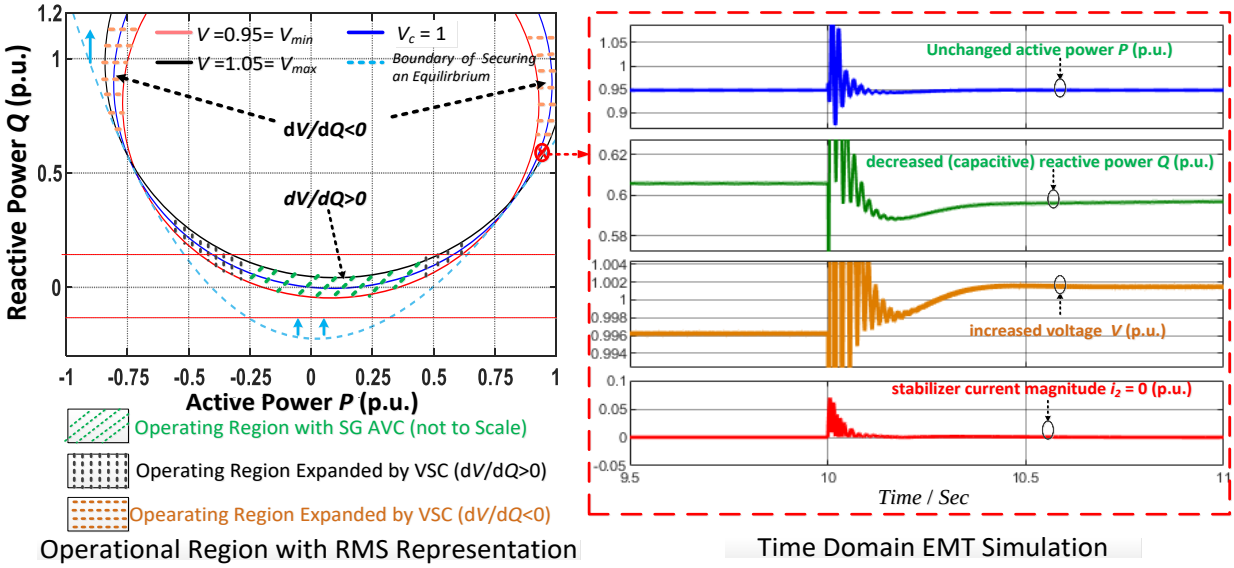

Fig. 4 Enhanced Transmission Limit with Remote VSC Stabilizer (*SCR* = 0.9, X/R = 10, Positive *P* as inversion)

station can be expanded to not only the region of $dV/dQ > S_{max} > 0$, but also region of $dV/dQ < 0$.

This effect is illustrated by an EMT simulation with *matlab*/*simulink* and classical average converter model. Based on the system configuration in Fig. 3, the parametric settings are listed in appendix. As shown in the simulated waveform in Fig. 4, the system started with a steady state operation from *Time* = 9.5 sec when VSC-HVDC station is inverting an active power of 0.95 p.u. with a VSC reactive power at 0.606 p.u. (capacitive, shunt compensation inclusive); the initial operating voltage at the VSC-HVDC terminal is 0.996 p.u. and the operating current of the VSC stabilizer is 0. At *Time* = 10 sec, an arbitrary reactive power step of 0.3% p.u. is applied to the VSC-HVDC. This step causes immediate oscillations and VSC stabilizer starts to output power to mitigate it. From *Time* = 10.5 sec, the system is back to steady state and the active power is back to the identical value before the step due to active power loop; the reactive power of VSC-HVDC, *Q*, has dropped to approximately 0.597 p.u.; however, the VSC-HVDC terminal voltage increases to 1.002 p.u. and the current of VSC stabilizer is back to zero at steady state. The corresponding operating point in RMS *Q*-*P* plane is marked as the red cross in the left half of Fig. 4.

In this example, the voltage increase caused by a drop of capacitive reactive power shows that with appropriate EMT stabilization, a transmission system is able operate in the region of negative dV/dQ despite of a positive var/volt droop is in place. This result illustrates a counter example against the forbidden region of Hoff bifurcation defined in RMS representations. In particular, it shows that the transmission limit set by negative voltage sensitivity against reactive power, dV/dQ, in RMS domain does not apply to converter domination. By pushing the limit of Hoff bifurcation further, EMT stabilization under converter domination can unlock a greater limit than synchronous machine and this can lead to a potential to exhaust the physical limit set against Saddle Node Bifurcation of the network.

This example further shows that the stabilization provided by the VSC stabilizer can be a promising solution to voltage stabilization due to 4 aspects: 1) The significant electrical distance between the VSC stabilizer and VSC-HVDC shows that VSC stabilization has a regional effect; 2) The zero-steady-state-current behaviour of the VSC stabilizer indicate a fairly low cost in the sizing of VSC stabilizer; 3) this zero-current consumption of stabilizer also means that the stabilization can be generally incorporated as a notch function of any VSC, e.g. VSC-HVDC, wind turbine, storage, etc., without affecting their original function in power conversion. 4) This autonomous stabilization structure and local measurement demonstrate a good potential in a low-inertia power system where centralized control becomes less practical.

V. Conclusion

Towards converter domination, the existing RMS methodologies of interpreting and assessing voltage instability is inadequate. EMT approaches must be used to assess the dynamics brought about by the interactions of converter control and electrical network. Comparing with synchronous machine, much faster measurement and fast actuation of converter domination can enable better damping with EMT quantities. With appropriate design in the EMT damping scheme, VSCs can break through the transmission limit set against Hoff bifurcation which is defined in RMS representations. VSC can enable power transmission entering the region of negative RMS voltage sensitivity to exploit the static limit set against non-existence of power flow equilibrium.

References

[1] John Pettigre, “National Grid’s Net Zero Commitment,” National Grid, Nov. 2019, access link: https://www.nationalgrid.com/stories/journey-to-net-zero/national-grids-net-zero-commitment.

[2] A. Bindra, “Projecting the evolution of power electronics: Highlights from FEPPCON VIII,” IEEE Power Electron. Mag., vol. 3, no. 1, pp. 32–44, 2016.

[3] P. Kundur, J. Paserba, V. Ajjarapu et al., “Definition and classification of power system stability IEEE/CIGRE joint task force on stability terms and definitions,” IEEE Trans. Power Syst., vol. 19, no. 3, pp. 1387–1401, 2004.

[4] Yong Tang, “Voltage Stability Analysis of Power System”. Springer, Singapore, p.p. 157, 2021

[5] P. Kundur, Power System Stability and Control. New York: McGraw-Hill, p.p.965, 1994.

[6] S. Grijalva, "Individual Branch and Path Necessary Conditions for Saddle-Node Bifurcation Voltage Collapse," IEEE Trans. on Pow. Syst., vol. 27, no. 1, pp. 12-19, Feb. 2012

[7] L. Xiong, X. Liu, Y. Liu and F. Zhuo, "Modeling and stability issues of voltage-source converter dominated power systems: A review," CSEE Journal of Power and Energy Systems, in press

[8] Anastasios Oulis Rousis, Goran Strbac, Noel Cunniffe, etl. “State-of-the-Art Literature: Review of System Scarcities at High Levels of Renewable Generation”, Technical Report of European Union’s Horizon 2020- EU-SysFlex, 2018

[9] K. Vu, M. M. Begovic, D. Novosel and M. M. Saha, "Use of local measurements to estimate voltage-stability margin," IEEE Trans. Pow. Syst., vol. 14, no. 3, pp. 1029-1035, Aug. 1999.

[10] P.A. Lof, G. Anderson, and D.J.Hill, “Voltage stability indices for stressed power systems,” IEEE Trans. on Pow. Syst., vol. 8, no. 1, pp. 326-335, Feb, 1993.

[11] V. Ajjarapu and C. Christy, “The continuation power flow: A tool for steady state voltage stability analysis,” IEEE Trans. on Pow. Syst., vol. 7, no. 1, pp. 416-423, Feb. 1992.

[12] B. Gao, G. K. Morison, and P. Kundur, “Voltage stability evaluation using modal analysis,” IEEE Trans. Pow. Syst., vol. 7, no. 4, pp. 1529-1542, Nov. 1992.

[13] V. A. Venikov, V. A. Stroev, V. I. Idelchick and V. I. Tarasov, "Estimation of electrical power system steady-state stability in load flow calculations," IEEE Trans. Power Apparatus and Systems, vol. 94, no. 3, pp. 1034-1041, May 1975

[14] Z. Zhang, D. Chen, K. Givaki and L. Xu, "A Less-Intrusive Approach to Stabilize VSC Transmission against Highly Variable Grid Strength," IEEE Journal of Emerging and Selected Topics in Power Electronics, in press

[15] J. H. Braslavsky, L. D. Collins and J. K. Ward, "Voltage Stability in a Grid-Connected Inverter With Automatic Volt-Watt and Volt-VAR Functions," IEEE Transactions on Smart Grid, vol. 10, no. 1, pp. 84-94, Jan. 2019.

[16] Q. Zhong, P. Nguyen, Z. Ma and W. Sheng, "Self-Synchronized Synchronverters: Inverters Without a Dedicated Synchronization Unit," IEEE Trans. Pow. Electron., vol. 29, no. 2, pp. 617-630, Feb. 2014.

[17] X. Zhang, D. Xia, Z. Fu, G. Wang and D. Xu, "An Improved Feedforward Control Method Considering PLL Dynamics to Improve Weak Grid Stability of Grid-Connected Inverters," IEEE Trans. Ind. App., vol. 54, no. 5, pp. 5143-5151, Sept.-Oct. 2018.

[18] X. Wang, J. Yao, J. Pei, P. Sun, H. Zhang and R. Liu, "Analysis and Damping Control of Small-Signal Oscillations for VSC Connected to Weak AC Grid During LVRT," IEEE Trans. on Energy Conv., vol. 34, no. 3, pp. 1667-1676, Sept. 2019.

APPENDIX

PARAMETRIC SETTINGS OF FIG. 3

Symbol	QUANTITY	Value
	Base voltage (instantaneous)	Rated phase voltage amplitude
	Base current (instantaneous)	$3/2 \times$ rated phase current amplitude
	Base power (p.u.)	VSC-HVDC rated power
V_s	grid voltage (p.u.)	1
SCR	Short circuit ratio at the terminal VSC-HVDC	0.9
X/R	*X/R* Ratio of the transmission line	10
L_1	VSC-HVDC AC Inductance (p.u.)	$0.2/(100\pi)$
R_1	VSC-HVDC resistance (p.u.)	0.005
L_2	VSC stablizer AC Inductance (p.u.)	$0.2/(100\pi)$
R_2	VSC-HVDC resistance (p.u.)	0.005
Q_{C1}	Shunt Capacitance of VSC-HVDC (p.u.)	0.1
Q_{C2}	Shunt Capacitance of VSC Stablizer (p.u.)	0.001
	Line Impedance between VSC-HVDC and Stabilizer (p.u.)	0.017+j0.17
	Line Impedance between VSC Stabilizer and grid source (p.u.)	0.094+j0.94
	Integral gain of PLL for both VSC (rad/p.u.)	$100\,\pi^2$
	Proportional gain of PLL for Both VSC (rad/p.u.)	20π
T_2, T_1	Constants of lead-lag compensator for both VSCs	0.2, 0.04
f	Frequency (Hz)	50
τ	aggregated delay of both VSC control (second)	1/5000
	Simulation time step (second)	1/10000